JCTC Journal of Chemical Theory and Computation

Article

pubs.acs.org/JCTC

Cumulant Approximated Second-Order Perturbation Theory Based on the Density Matrix Renormalization Group for Transition Metal Complexes: A Benchmark Study

Quan Manh Phung,[†] Sebastian Wouters,[‡] and Kristine Pierloot*[,†]

[†]Department of Chemistry, KU Leuven, Celestijnenlaan 200F, 3001 Leuven, Belgium

[‡]Center for Molecular Modelling, Ghent University, Technologiepark 903, 9052 Zwijnaarde, Belgium

Supporting Information

ABSTRACT: The complete active space second order perturbation theory (CASPT2) can be extended to larger active spaces by using the density matrix renormalization group (DMRG) as solver. Two variants are commonly used: the costly DMRG-CASPT2 with exact 4-particle reduced density matrix (4-RDM) and the cheaper DMRG-cu(4)-CASPT2 in which the 4-cumulant is discarded. To assess the accuracy and limitations of the latter variant DMRG-cu(4)-CASPT2 we study the spin state energetics of iron porphyrin Fe(P) and its model compound FeL_2, a model for the active center of NiFe hydrogenase, and manganese-oxo porphyrin $MnO(P)^+$; a series of excited states of chromium hexacarbonyl $Cr(CO)_6$; and the interconversion of two $Cu_2O_2^{2+}$ isomers. Our results clearly show that PT2 on top of DMRG is essential in order to obtain quantitative results for transition metal complexes. Good results were obtained with DMRG-cu(4)-CASPT2 as compared to full CASPT2 and DMRG-CASPT2 in calculations with small- and medium-sized active spaces. In calculations with large-sized active spaces (~30 active orbitals), the performance of DMRG-cu(4)-CASPT2 is less impressive due to the errors originating from both the finite number of renormalized states m and the 4-RDM approximation.

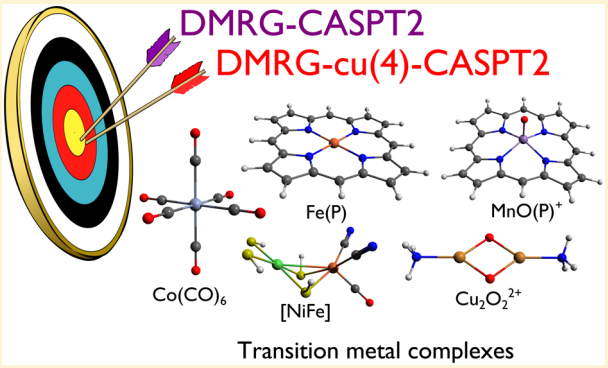

1. INTRODUCTION

The density matrix renormalization group (DMRG), first introduced by White in 1992,[1,2] is considered one of the most promising methods to study strongly correlated molecular systems.[3] Among different novel computational techniques, DMRG has several unique features. Because of its compact parametrization of the wave function, known as the matrix product state MPS,[4] DMRG is an efficient alternative for full configuration interaction (FCI) and multiconfigurational methods such as the complete active space self-consistent field (CASSCF). Its accuracy depends on a single tunable parameter, the number of renormalized states m. In some applications such as water,[5] N_2,[6] or Be_2,[7] it was shown that DMRG can converge to the exact FCI limit at a large m value. Because the MPS wave function in DMRG is not based on an excitation expansion from a single-reference, DMRG is also extremely useful to study strongly correlated systems, including transition metal (TM) complexes. With a polynomial scaling, DMRG can handle much larger active spaces as compared to conventional CASSCF, allowing one to study large TM systems with 30−50 active orbitals.[3] DMRG has already been successfully applied to study various problems in TM chemistry,[8−22] starting from the energetic properties of small TM complexes and clusters such as CoH and Cu_2O_2 by Marti et al.,[10] to electronic properties of large mononuclear TM complexes such as the manganese-salen complex[20] and an iron-oxo porphyrin system,[22] and also for multinuclear TM complexes such as the Mn_4Ca cluster in photosystem II,[15] or for [4Fe-4S] biological iron−sulfur complexes.[17] Last but not least, by measuring quantum entanglement based on the von Neumann entropy (a well-known concept in quantum information theory), DMRG can provide valuable insights into the correlation picture of a wave function. By analyzing the single-orbital entropy[23] and the mutual information $I_{i,j}$,[14,24] it is possible to quantify the amount of static and dynamic correlation in a wave function,[14] to study a bond-breaking reaction,[24,25] or to systematically select orbitals for the active space.[26]

Despite many successful applications, there are two main problems with DMRG: (a) it is (even) less "black-box" than the traditional CAS method and (b) it only includes static correlation and inefficiently treats dynamic correlation. In DMRG, an additional set of technical parameters was introduced affecting convergence and accuracy. These parameters include the number of renormalized states m, the choice

Received: July 18, 2016
Published: August 22, 2016

DOI: 10.1021/acs.jctc.6b00714
J. Chem. Theory Comput. 2016, 12, 4352−4361

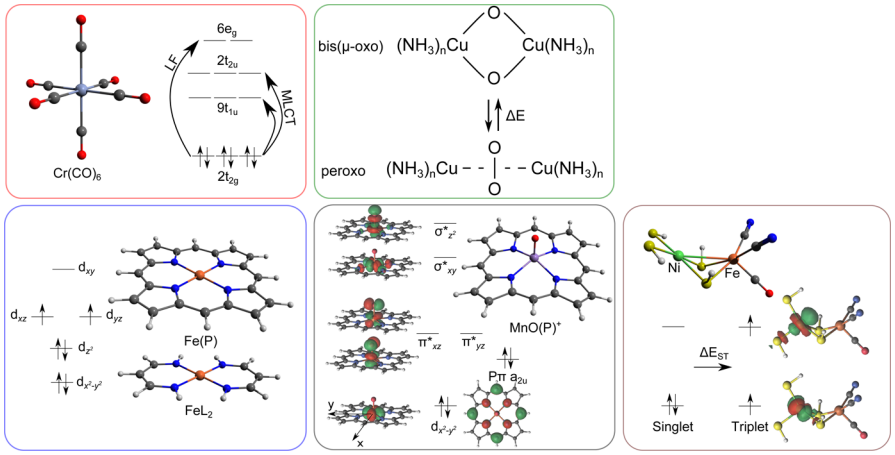

Figure 1. Graphical abstract of problems investigated in this work: spin state energetics of iron porphyrin Fe(P) (P = $C_{20}N_4H_{12}^{2-}$) and its model FeL_2 (L = $C_3N_2H_5^-$), NiFe hydrogenase model $[(SH)_2Ni(SH)_2Fe(CO)(CN)_2]^{2-}$, and manganese-oxo porphyrin $MnO(P)^+$; excited states of chromium hexacarbonyl $Cr(CO)_6$; and the interconversion of two $Cu_2O_2^{2+}$ isomers.

and ordering of the orbitals in the active space, and the initialization procedure of the matrix product state MPS (the so-called warm-up sweep). First, the number of renormalized states m determines the DMRG accuracy, together with its computational cost: DMRG CPU time and memory scale as $O(m^3a^3 + m^2a^4)$ and $O(m^2a^2)$,[3] respectively, a being the number of active orbitals. Thus, m must be properly chosen so that converged results are obtained at a reasonable computational cost. Second, the MPS is not invariant to orbital rotations within the active space. A good orbital ordering should have low quantum entanglement (e.g., by minimizing the entanglement distance $I_{\text{dist}} \sim \sum_{i,j} I_{i,j}|i-j|^2$). This can be done by putting highly entangled orbitals close to each other, which can significantly enhance the DMRG accuracy. Some heuristic algorithms of orbital ordering are available: Fiedler vector order[27] or genetic algorithm order.[28] Finally, because of its compact parametrization, a DMRG solution can be easily trapped in a "local minimum". This can be avoided by using a suitable guess in the warm-up sweep, such as a configuration interaction based extended active space (CI-DEAS) procedure,[23] or by adding a small amount of perturbative noise into the wave function.[29]

With a sufficiently large active space, DMRG can easily describe static electron correlation. However, dynamic correlation is insufficiently treated by DMRG. The lack of dynamic correlation is currently the biggest problem of DMRG. Inspired by conventional *ab initio* methods, perturbative approaches on top of the MPS wave function such as CASPT2[30−33] or NEVPT2[34−40] might be used to account for dynamic correlation. The key components to obtain the PT2 energy are the n-particle reduced density matrices (n-RDMs), with n = 1−4. In a naïve implementation, the cost of an n-RDM calculation scales as a^{2n}, thus 4-RDM (and even 3-RDM) calculations become the bottleneck in DMRG-PT2. Three solutions have been proposed and (very) recently implemented. The first one is to avoid calculations of the 4-RDM by using a cumulant reconstruction based on the 3-RDM, in which the 4-cumulant is neglected. This approximation, denoted as DMRG-cu(4)-CASPT2,[32] has so far only been used in some studies of Yanai et al.[22,32,41] The authors showed that in some systems DMRG-cu(4)-CASPT2 gives reasonable results, while a further approximation which additionally neglects the 3-cumulant (cu(3,4)) fails dramatically. The main problem with this method is that the energy denominators in the CASPT2 expression are not exactly evaluated, which might give too small denominators (so-called "false" intruder states[32,42]) and an instability of the CASPT2 energy. Thus, more investigations should be done in order to assess the accuracy of this method. The second solution avoids the computation of the full 4-RDM by working in the pseudocanonical basis.[31] Because a nonoptimal choice of active space orbitals is used for DMRG, very large m values can be required to achieve acceptable convergence. The third solution, the so-called MPS-NEVPT2,[37] is promising, as it bypasses the need to calculate the 3- and 4-RDM, with the trade-off that it requires many parallel DMRG calculations to solve for parts of the first-order wave function. Thus, with the third option one could perform large active space calculations without the problem of calculating the 3- and 4-RDM.

In this work, we study the accuracy and limitations of the DMRG-cu(4)-CASPT2 method (hereafter called cu(4)-CASPT2[m]) for a series of important chemical properties in transition metal complexes, shown in Figure 1: spin state energetics of iron porphyrin Fe(P) and its model compound FeL_2, a model for the active center of NiFe hydrogenase, and manganese-oxo porphyrin $MnO(P)^+$; a series of excited states of chromium hexacarbonyl $Cr(CO)_6$; and the interconversion of two $Cu_2O_2^{2+}$ isomers. These problems have already been studied before by us[43−46] with conventional CASSCF/CASPT2 and its extension RASSCF/RASPT2. The results obtained here will be compared with our previous works wherever possible.[47] With active spaces containing more than 18 orbitals, CASSCF/CASPT2 calculations are computationally prohibited. Thus, we used DMRG-CASPT2 (with an efficient contraction of the generalized Fock matrix with the 4-RDM) implemented in CheMPS2.[20,33,48,49] Since there is no approximation in the 4-RDM, DMRG-CASPT2 (hereafter called CASPT2[m]) should converge to regular CASPT2 at large enough m values. The results in this benchmark work allow us to estimate the reliability of cu(4)-CASPT2 as compared to CASPT2, for future practical purposes i.e. to study large transition metal complexes with large active space using a low-cost cu(4)-CASPT2[m] with moderate m.

DOI: 10.1021/acs.jctc.6b00714
J. Chem. Theory Comput. 2016, 12, 4352−4361

2. COMPUTATIONAL DETAILS

All calculations with multiconfigurational perturbation theory CASSCF/CASPT2[30] were performed with the MOLCAS-8 program,[50] while the cu(4)-CASPT2[m] calculations were done with the BLOCK program[3,12,29,51−53] interfaced with MOLCAS. The cu(4)-CASPT2 calculations were done in two steps. In the first step, n-RDMs with n = 2,3 were calculated with the BLOCK code. In the subsequent step, approximations of the 4-RDM were estimated, followed by a CASPT2 calculation with MOLCAS. The cu(4)-CASPT2 results are compared with the full CASPT2 (or CASPT2[m] done by CHEMPS2[20,33,48,49]) results, allowing us to assess the accuracy of the 4-RDM cumulant approximation.

In all calculations, extensive relativistic atomic natural orbital (ANO-RCC) type basis sets were employed. The contractions are [7s6p5d3f2g1h] for the metal atom,[54] [5s4p2d1f] on S, [4s3p2d1f] on C,[47] N, O,[55] and [3s1p] on H.[56] Scalar relativistic effects were included using a standard second-order Douglas-Kroll-Hess (DKH) Hamiltonian.[57−59] In all PT2 calculations, all valence electrons were correlated, including also the 3s and 3p electrons of the metal atoms. All PT2 calculations were performed with the standard ionization potential electron affinity (IPEA) Hamiltonian[60] of 0.25 au. In all CASPT2 and cu(4)-CASPT2 calculations, an imaginary level shift of 0.1 au[61] was used to avoid weak intruder states and improve convergence of the perturbational treatment. In the cu(4)-CASPT2 calculations with small active spaces (FeL_2 and Fe(P)), "false" intruder states emerge preventing convergence of the PT2 calculations, hence the imaginary shift was increased to 0.2 au. Cholesky decomposition of the electron repulsion integral with a threshold of 10^{-6} au[62] was used to reduce computational times and disk storage needs.

The active spaces are different for each molecule and will therefore be presented in the appropriate section of the results. We describe here the notation to label the CASSCF and DMRG active spaces. For the CASSCF calculations, we used the traditional notation CAS(n,a), where n is the number of electrons included in the active space and a is the number of active orbitals. In the DMRG calculations, we used a similar notation DMRG(n,a)[m] where m is the number of renormalized states. In all DMRG calculations, we start with a small m and increase m until cu(4)-CASPT2[m] relative energies converge within 0.5−1 kcal/mol. This convergence threshold is smaller than the typical CASPT2 error of TM complexes of around 0.1−0.3 eV (2.3−7 kcal/mol).

All DMRG calculations were done with the spin-adapted DMRG algorithm.[12,20] In order to fully investigate different electromers, molecular symmetry was maintained, and consequently delocalized natural orbitals were used in all DMRG calculations. In order to avoid poor convergence during the warm-up sweep, the orbital ordering was automated by minimizing the quantum entanglement using either Fiedler[27] or a genetic algorithm (GA).[28] The quantum entanglement between the two orbitals i and j is simply estimated by the exchange integral $K_{ij} = \int\int d\mathbf{r}_1 d\mathbf{r}_2 r_{12}^{-1} \phi_i^*(\mathbf{r}_1)\phi_j(\mathbf{r}_2)\phi_j^*(\mathbf{r}_1)\phi_i(\mathbf{r}_2)$, which indicates proximity and spatial overlap of i and j. We used the default sweep schedule implemented in BLOCK, i.e. initial DMRG sweeps were done with small m values to approximately converge the DMRG wave function while later sweeps were carried out with a larger m. Moreover, a small amount of perturbative noise $\epsilon = 1 \times 10^{-4}$ (in BLOCK) was added into the wave function in the warm-up sweep to prevent the DMRG algorithm from being trapped at a local minimum. The calculations performed in this work are single-point calculations using DFT structures taken from previous studies.[43,45,46,63] For $Cr(CO)_6$, the calculations were performed using the experimental octahedral structure.[64]

3. RESULTS AND DISCUSSION

3.1. Spin State Energetics of FeL_2 and Fe(P): Small-Sized Active Space. Because of its diverse biological functions, Fe(II) porphyrin Fe(P) has already for many years been the subject of experimental[65−72] and theoretical studies.[44,63,73−80] The electronic structure of Fe(P) is well-defined. Experimental data of tetraphenylporphinatoiron(II) FeTPP[65] and octaethylporphinatoiron(II) FeOEP[67,68] from different techniques pointed to a triplet ground state. High-quality theoretical results from CASPT2(16,15)[44] and CCSD-(T)[63] indicate that the ground state is $^3A_{2g}$ (D_{4h} symmetry).

In this section, we present the spin state energetics of Fe(P) and its mimic model FeL_2. As illustrated in Figure 2, four

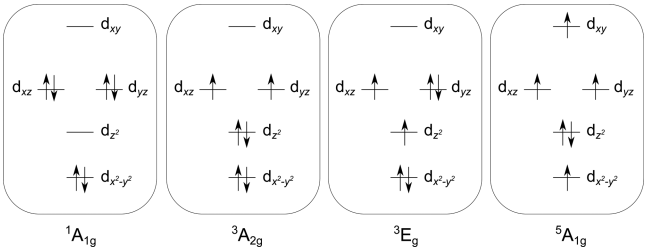

Figure 2. Four states of Fe(P) investigated in this work. The point group symmetry is D_{4h} (D_{2h} for ^3E_g), and the N ligands are placed between the x and y axes.

electromeric states of Fe(P) were studied: $^1A_{1g}$, ^3E_g, $^3A_{2g}$, and $^5A_{1g}$. In FeL_2 (D_{2h} symmetry) we studied four corresponding electromeric states with the same electron configuration, i.e. ^1A_g, $^3B_{1g}$, $^3B_{3g}$, and ^5A_g. In both FeL_2 and Fe(P), the active spaces consist of 11 orbitals including the Fe 3d orbitals, a set of five 3d′ orbitals to describe the 3d double shell effect, and one Fe−N σ bonding orbital. Different m values were used, starting from a tiny m = 10, to a relatively large m = 1000.

The DMRG-SCF and cu(4)-CASPT2 results of FeL_2 and Fe(P) are shown in Tables 1 and 2. The errors of cu(4)-CASPT2 as compared to CASPT2 are summarized in Figure 3. It can be seen that at a large m value, cu(4)-CASPT2 can well-reproduce the CASPT2 relative energies. At m = 1000, the errors of cu(4)-CASPT2 as compared to CASPT2 in FeL_2 are negligible, less than 0.3 kcal/mol. For Fe(P), the errors are even smaller, less than 0.1 kcal/mol for all states. The errors are still negligible even at a much smaller m = 50. This shows that the 4-RDM reconstruction introduces minor errors to the PT2 solution and indicates that cu(4)-CASPT2 is a very good approximation of CASPT2. Moreover, the similarity between the FeL_2 and Fe(P) results shows that the cu(4)-CASPT2 error is independent from the molecular size (when the same active space is used).

Comparing between the results at different m, we can conclude that a converged cu(4)-CASPT2 result (within 0.1 kcal/mol) can be obtained when the corresponding reference DMRG-SCF energy converges within 0.1 kcal/mol (by using a large enough m value). At a too small m value, e.g. m = 10, the DMRG-SCF errors can be as large as 1.5 kcal/mol,

DOI: 10.1021/acs.jctc.6b00714
J. Chem. Theory Comput. 2016, 12, 4352−4361

Table 1. Relative Energies (kcal/mol) of the Low-Lying Electronic States of FeL_2 Calculated with DMRG-SCF(8,11)[m] and cu(4)-CASPT2(8,11)[m], in Comparison with CASSCF and CASPT2 Results[b]

	^1A_g		$^3B_{1g}$		$^3B_{3g}$	
m	SCF	PT2[a]	SCF	PT2[a]	SCF	PT2[a]
10	56.0	41.1	20.5	0.7	22.8	−1.0
20	54.8	39.8	19.5	−0.4	21.6	−2.3
30	54.8	39.7	19.2	−0.9	21.4	−2.5
40	54.8	39.7	19.0	−0.6	21.3	−2.7
50	54.8	39.7	19.0	−0.7	21.3	−2.8
100	54.8	39.7	18.9	−0.8	21.3	−2.9
400	54.8	39.8	18.9	−0.7	21.3	−2.7
800	54.8	39.7	18.9	−0.7	21.3	−2.8
1000	54.8	39.7	18.9	−0.7	21.3	−2.8
CAS	54.8	39.9	18.9	−1.0	21.3	−3.0

[a]cu(4)-CASPT2 calculations were done with an imaginary shift of 0.2 au. [b]The ^5A_g state is the reference.

Table 2. Relative Energies (kcal/mol) of the Low-Lying Electronic States of Fe(P) Calculated with DMRG-SCF(8,11)[m] and cu(4)-CASPT2(8,11)[m], in Comparison with CASSCF and CASPT2 Results[c]

	$^1A_{1g}$		^3E_g		$^3A_{2g}$	
m	SCF	PT2[a]	SCF	PT2[a]	SCF	PT2[a]
10	48.8	42.1	20.1	8.7	18.3	6.3
20	48.0	41.2	18.8	7.4	16.9	5.2
30	47.3	40.0	18.7	7.1	16.7	5.1
40	47.3	39.8	18.6	6.9	16.5	5.1
50	47.3	39.8	18.6	6.9	16.5	5.0
100	47.2	39.8	18.5	6.9	16.4	5.0
400	47.2	39.8	18.5	6.9	16.4	4.9
800	47.2	39.9	18.5	7.0	16.4	5.0
1000	47.2	39.8	18.5	6.9	16.4	4.9
CAS	47.2	39.8	18.5	6.9	16.4	4.8
CAS[b]		37.1		4.2		2.1

[a]cu(4)-CASPT2 calculations were done with an imaginary shift of 0.2 au. [b]CASSCF/CASPT2 results from ref 44. [c]The $^5A_{1g}$ state is the reference.

consequently, the cu(4)-CASPT2 errors are 1.7 kcal/mol in FeL_2 and 2.3 kcal/mol in Fe(P).

Because cu(4)-CASPT2 is just an approximation to CASPT2, it inherits all of the weaknesses of CASPT2, including a typical error for spin state energetics of around 2−5 kcal/mol.[63,73,81] Thus, both cu(4)-CASPT2 and CASPT2 falsely predict that $^5A_{1g}$ is the ground state, in contradiction with the experimental result ($^3A_{2g}$). This error could be traced back to an inaccurate description of the Fe semicore (3s,3p) correlation by PT2, which will be addressed in a future work.[82] We also note here that there are differences of ∼2.7 kcal/mol between the CASPT2 results and our previous CASPT2[44] employing the same active space. The reason for this difference is that a different (and faulty) C basis set was used in the previous work. The best computational results available were obtained in a recent CCSD(T) study: 29.9, − 0.6, and −2.3 kcal/mol for $^1A_{1g}$, ^3E_g, and $^3A_{2g}$, respectively.[63]

3.2. Electronic Absorption Spectrum of $Cr(CO)_6$: Medium-Sized Active Space. The UV gas phase absorption spectra of $Cr(CO)_6$ and other metal carbonyl complexes have been intensively used in benchmarking studies of different theoretical methods, such as time-dependent DFT,[83,84] CASPT2,[85] RASPT2,[44] and coupled-cluster methods.[86] $Cr(CO)_6$ has an octahedral structure with a closed-shell $^1A_{1g}$ ground state corresponding to the configuration $2t_{2g}^6 6e_g^0$. In the spectrum of $Cr(CO)_6$,[87] two intense bands at 4.44 and 5.48 eV were assigned as charge-transfer excitations from $2t_{2g}$ into the $9t_{1u}$ and $2t_{2u}$ CO π^* shells ($^1A_{1g} \rightarrow {}^1T_{1u}$). In order to describe these transitions, a minimum active space should contain the Cr 3d orbitals ($2t_{2g}^6$ and $6e_g^0$) and their bonding $5e_g$ and antibonding $3t_{2g}$ ligand counterparts, as well as six π^* orbitals $9t_{1u}$ and $2t_{2u}$ of CO. This leads to an active space of 10 electrons in 16 orbitals. With this active space, we study here six excited states in the vertical spectrum of $Cr(CO)_6$, aiming at assessing the accuracy of cu(4)-CASPT2 as compared to CASPT2 for the calculation of excited states. The six excited states include four metal-to-ligand charge transfer (MLCT) states a,b$^1T_{1u}$ and a,b$^1T_{2u}$, corresponding to excitations from $2t_{2g}$ into $9t_{1u}$ and $2t_{2u}$, and two ligand field (LF) states $^1T_{1g}$ and $^1T_{2g}$, corresponding to excitations from $2t_{2g}$ into $6e_g$. State-average calculations were performed in the same way as described in ref 44.

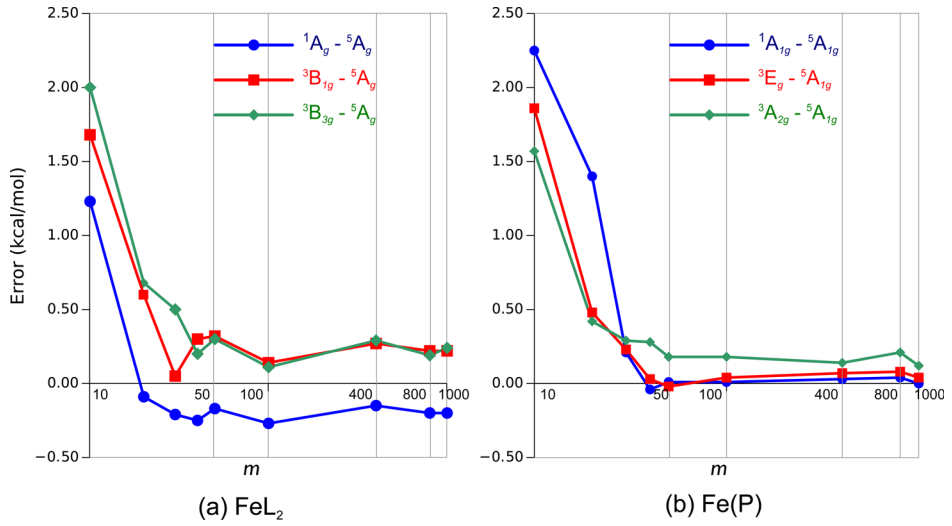

Figure 3. cu(4)-CASPT2 errors (in kcal/mol) as compared to CASPT2 for spin state energetics of (a) FeL_2 and (b) Fe(P).

DOI: 10.1021/acs.jctc.6b00714
J. Chem. Theory Comput. 2016, 12, 4352−4361

Table 3. Relative Energies of the Low-Lying Excited State in $Cr(CO)_6$ Calculated with DMRG-SCF(10,16)[m] and cu(4)-CASPT2(10,16)[m], in Comparison with CASSCF, CASPT2 Results, and Experimental Data

	$^1T_{1g}$		$^1T_{2g}$		a^1T_{2u}		a^1T_{1u}		b^1T_{2u}		b^1T_{1u}	
m	SCF	PT2[a]	SCF	PT2[a]	SCF	PT2[a]	SCF	PT2[a]	SCF	PT2[a]	SCF	PT2[a]
100	6.13	*b*	6.84	4.97	5.69	*b*	6.42	*b*	6.92	*b*	8.17	*b*
200	6.05	4.94	6.76	5.40	5.62	3.87	6.34	4.47	6.84	4.84	8.08	5.23
400	5.97	4.88	6.72	5.49	5.60	4.13	6.31	4.59	6.81	4.95	8.05	5.43
1000	5.96	5.15	6.71	5.55	5.59	4.18	6.30	4.59	6.80	4.95	8.04	5.37
1500	5.96	5.13	6.71	5.51	5.59	4.14	6.30	4.56	6.80	4.92	8.04	5.39
2000	5.96	5.11	6.71	5.50	5.59	4.13	6.30	4.55	6.80	4.91	8.04	5.41
CAS	5.96	4.94	6.71	5.37	5.59	4.00	6.30	4.44	6.80	4.82	8.04	5.29
CAS[c]		4.92		5.35		3.88		4.31		4.68		5.16
exp.[d]								4.44				5.48

[a]cu(4)-CASPT2. [b]cu(4)-CASPT2[100] calculations are not converged. [c]Reference 44, using a different C basis set.[47] [d]From ref 88.

In Table 3, we present the excitation energies of the six excited states of $Cr(CO)_6$ calculated with DMRG-SCF(10,16)[m] and cu(4)-CASPT2(10,16)[m], in comparison with CASSCF and CASPT2 results. The errors of cu(4)-CASPT2 (in eV) with respect to CASPT2 are plotted in Figure 4. With

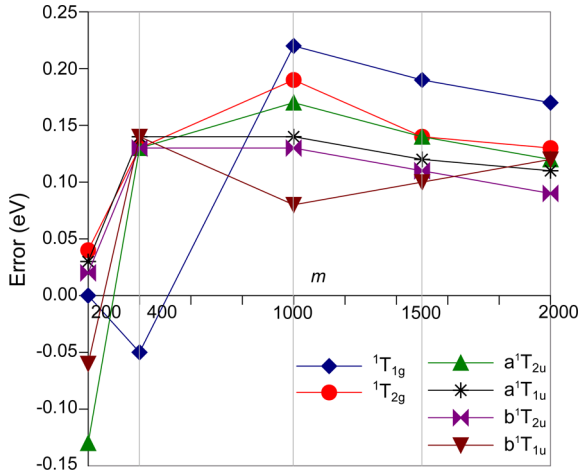

Figure 4. cu(4)-CASPT2 errors (in eV) compared to CASPT2 for the excited states of $Cr(CO)_6$.

medium-sized active spaces, a calculation with a too small m can either be trapped at a local minimum or converge to a wrong electronic state, leading to wrong DMRG-SCF and cu(4)-CASPT2 results. Thus, only calculations with m larger than 100 were done.

In contrast to the calculations of FeL_2 and Fe(P), the performance of cu(4)-CASPT2 is quite poor, i.e. cu(4)-CASPT2 slowly converges with respect to m. At m = 100, the DMRG reference is poorly produced, leading to diverged cu(4)-CASPT2 results. The only result at m = 100 we can obtain is for the $^1T_{2g}$ state, with an error of 0.54 eV as compared to cu(4)-CASPT2[1500]. Even at a relatively high m value (1000), giving well-converged DMRG-SCF results, there are still non-negligible differences of 0.04−0.05 eV (up to 1 kcal/mol) with respect to cu(4)-CASPT2[2000]. Moreover, the best cu(4)-CASPT2 results at m = 2000 are still too high by 0.1−0.2 eV (up to 5 kcal/mol) as compared to CASPT2. This seems discouraging since in the previous test of FeL_2 and Fe(P) with smaller active spaces, remaining errors were less than 0.3 kcal/mol. However, considering that the energy differences between the ground state and the excited states are large (4.0−5.5 eV), errors of 0.1−0.2 eV might still be considered acceptable. We also note that cu(4)-CASPT2[1500] still yields good results as compared to experiment, with errors of ∼0.1 eV. As was shown in a previous RASPT2 study,[44] the errors can be further reduced by using a larger active space containing an extra 3d′ shell as well as extra CO π^* orbitals.

3.3. Singlet−Triplet Energy Difference for Active-Site Models of [NiFe] Hydrogenase: Medium-Sized Active Space. The hydrogenases are a group of enzymes catalyzing the reversible conversion of H_2 to protons and electrons. [NiFe] hydrogenase, containing a Ni and an Fe ion, has extensively been investigated both by experimental and theoretical methods.[45,89−94] It has been widely accepted that at the catalytically active state (Ni-SIa), the Fe ion is low-spin Fe^{2+}, while the spin state of the Ni^{2+} ion has long been the subject of debate. Recently, we provided a benchmark study[45] of several models of the [NiFe] hydrogenases using different density functionals and *ab initio* techniques such as CASPT2, RASPT2, and CCSD(T). Our results suggest a singlet ground state of Ni-SIa both in gas phase and in a protein environment. In this section, we re-evaluate the singlet−triplet energy difference using cu(4)-CASPT2, in order to investigate the accuracy of this method. We only perform calculations using vacuum-optimized structures with C_s symmetry: the singlet state is $^1A'$, whereas the triplet state is $^3A''$, with their respective structures shown in Figure 5.

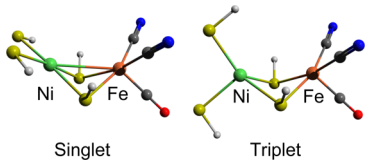

Figure 5. Geometry of the singlet state with square-planar and triplet state with tetrahedral Ni^{2+}.

The calculations were done with medium-sized active spaces, CAS(20,21) for the singlet state and CAS(22,22) for the triplet state. The active spaces (described in ref 45) contain all 3d orbitals of both Ni and Fe and a set of five Ni 3d′ and three Fe 3d′ to account for the double-shell effect, as well as a set of bonding orbitals between the metal atoms and the ligands (three orbitals in the singlet state and four in the triplet state).

The energy difference between the singlet and triplet states $\Delta E_{ST} = E_{triplet} - E_{singlet}$ calculated with cu(4)-CASPT2 is presented in Table 4. Since CASSCF/CASPT2 calculations are

DOI: 10.1021/acs.jctc.6b00714
J. Chem. Theory Comput. 2016, 12, 4352−4361

Table 4. $^1A'$-$^3A''$ Energy Difference (in kcal/mol) in the [NiFe] Model Calculated with DMRG-SCF[m] and cu(4)-CASPT2[m], in Comparison with CASPT2[m], RASPT2, and CCSD(T)

m	DMRG-SCF	cu(4)-CASPT2	CASPT2[a]	CCSD(T)[b]	RASPT2(SDTQ)[b]	RASPT2(SDTQ5)[b]
100	−16.1	17.4				
200	−15.9	16.9				
400	−15.8	15.9				
1000	−15.8	15.2	14.7			
1500	−15.8	15.4	14.7			
				13.6	11.5	12.0

[a]CASPT2[m] (exact 4-RDM) results from CheMPS2.[33] [b]From ref 45 with slightly smaller basis sets of Ni and Fe [7s6p4d3f2g1h].

computationally prohibited with this active space, cu(4)-CASPT2 results are compared with CASPT2[m] calculated with the CheMPS2 code. As the 4-RDM is exactly calculated in CheMPS2, CASPT2[m] should be equal to CASSCF/CASPT2 when a sufficiently large m is used. Indeed, the ΔE_{ST} value at m = 1000 is already converged. We expect that ΔE_{ST} at the CASSCF/CASPT2 level is very close to 14.7 kcal/mol. cu(4)-CASPT2 predicts a similar ΔE_{ST} result, 15.2 kcal/mol at m = 1000 and 15.4 kcal/mol at m = 1500. The small difference, less than 1 kcal/mol, between cu(4)-CASPT2[1500] and CASPT2[1500] indicates that the approximated 4-RDM is sufficiently reliable. Additionally, both cu(4)-CASPT2[1500] and CASPT2[1500] results are in good agreement with CCSD(T), within 2 kcal/mol. We also note that the difference between CASPT2[1500] and our previous RASPT2(SDTQ) (up to quadruple excitation level in RASSCF) result[45] (11.5 kcal/mol) using the same active space is rather large (3.2 kcal/mol). This difference is slightly decreased to 2.7 kcal/mol when the excitation level in the RASSCF was increased to five and should be smaller using higher excitations or moving active orbitals from RAS1 and RAS3 to RAS2. Nevertheless, all four methods cu(4)-CASPT2, CASPT2, RASPT2, and CCSD(T) predict a singlet ground state for the [NiFe] model.

3.4. The Interconversion of Two Isomers of $Cu_2O_2^{2+}$ Models: Medium-Sized Active Space. The interconversion between the bis(μ-oxo) and peroxo forms of $Cu_2O_2^{2+}$ (see Figure 1) has been extensively investigated by many theoretical methods such as CR-CC(2,3),[43] CASSCF/CASPT2,[95] and RASSCF/RASPT2,[43] as well as numerous DMRG calculations.[8,9,26,27] Since throughout this work we systematically employed the ANO-RCC basis sets, with scalar relativistic corrections from the Douglas-Kroll-Hess Hamiltonian, and semicore (3s,3p) electron correlation correction, it is difficult to compare our results with previous studies using different basis sets and active spaces. Our goal in this section is primarily to compare the performance of cu(4)-CASPT2 with CASPT2 employing a medium-sized active space, i.e. 24 electrons in 24 orbitals. We chose an active space including the most important correlation effects related to the Cu−O bonds and the Cu 3d double-shell effect, consisting of ten Cu orbitals (3d, 3d′) and four O orbitals ($2p_x$, $2p_y$). We mention here this active space is still not capable of providing quantitative results. This was pointed out in a previous RASPT2 study,[43] showing that a minimum active space containing 28−32 orbitals is needed for that purpose.

In Table 5, we present the relative energies between the bis(μ-oxo) and peroxo isomers of $Cu_2O_2^{2+}$ and $[Cu(NH_3)]_2O_2^{2+}$ ($\Delta E = E_{bis} - E_{per}$), calculated with DMRG-SCF, cu(4)-CASPT2, and CASPT2[m]. It is expected that CASPT2[m] with a sufficiently large m gives the most accurate results, which are 23.2 and 22.6 kcal/mol for $Cu_2O_2^{2+}$ and $[Cu(NH_3)]_2O_2^{2+}$, respectively. These numbers are used as a reference. The results with cu(4)-CASPT2 indicate that the relative energies converge rather fast with respect to m. Even cu(4)-CASPT2[100] can give satisfactory results, with an error of only 0.5−0.6 kcal/mol compared to cu(4)-CASPT2[1500]. The difference between cu(4)-CASPT2[1500] and CASPT2[1500] is negligible, less than 0.1 kcal/mol in $Cu_2O_2^{2+}$ and about 0.4 kcal/mol in $[Cu(NH_3)]_2O_2^{2+}$. As compared to the previous sections, in which we presented the spin state energetics of TM complexes, the cu(4)-CASPT2 performance is excellent, probably because the problem considered here does not involve a spin change between the isomers. The results again indicate that the 4-RDM approximation in cu(4)-CASPT2 is independent from the molecular size if similar active spaces are selected.

Table 5. Relative Energies (in kcal/mol) of the Bis(μ-oxo) and Peroxo Structures of $Cu_2O_2^{2+}$ and $[Cu(NH_3)]_2O_2^{2+}$ $\Delta E = E_{bis} - E_{per}$, Calculated with DMRG-SCF[m] and cu(4)-CASPT2[m], in Comparison with CASPT2[m]

m	DMRG-SCF	cu(4)-CASPT2	CASPT2[a]
$Cu_2O_2^{2+}$			
100	35.0	23.8	
200	35.0	23.3	
400	35.1	23.1	
1000	35.1	23.0	23.0
1500	35.1	23.1	23.2
$[Cu(NH_3)]_2O_2^{2+}$			
100	19.8	22.7	
200	19.6	22.4	
400	19.6	21.8	
1000	19.5	22.1	22.6
1500	19.5	22.2	22.6

[a]CASPT2[m] (exact 4-RDM) results from CheMPS2.[33]

3.5. Manganese-Oxo Porphyrin $MnO(P)^+$: Medium- and Large-Sized Active Spaces. The high-valent Mn-oxo complex $MnO(P)^+$ has received ample attention[96] because of its ability to catalyze oxygen atom transfer (OAT) reactions. In its low-spin (S = 0) ground state,[97−99] this complex shows a remarkable stability[100] and a low oxyl character in the Mn−O axial oxygen.[101,102] This might be the reason for the inertness toward OAT of the singlet state. Jin and Groves[98] therefore proposed that release of oxygen from $MnO(P)^+$ should rather proceed via (a) thermally accessible reactive high-spin (triplet or quintet) state(s). In a recent paper,[46] we confirmed this idea by investigating the spin state energetics and oxyl character of important low-lying states in Mn-oxo porphyrin $MnO(P)^+$ using CASPT2 and RASPT2. In this section, we aim at reproducing and improving the results of our previous study[46]

DOI: 10.1021/acs.jctc.6b00714
J. Chem. Theory Comput. 2016, 12, 4352−4361

using cu(4)-CASPT2. An overview of the considered states is provided in Table 6.

Table 6. Six States of $MnO(P)^+$ Investigated in This Work

		$Mn(3d_\delta)$[a]	$P(\pi a_{1u})$	$P(\pi a_{2u})$	π^*_{xz}	π^*_{yz}
$^1Mn^{V}O(P)$	$^1A_1$	↑↓	↑↓	↑↓		
$^3Mn^{V}O(P)$	$^3B_1$	↑	↑↓	↑↓		↑
$^5Mn^{IV}O(P^{\bullet}a_{2u})$	$^5A_2$	↑	↑↓	↑	↑	↑
$^3Mn^{IV}O(P^{\bullet}a_{2u})$	$^3B_1$	↑↓	↑↓	↑	↑	
$^5Mn^{IV}O(P^{\bullet}a_{1u})$	$^5A_2$	↑	↑	↑↓	↑	↑
$^3Mn^{IV}O(P^{\bullet}a_{1u})$	$^3B_1$	↑↓	↑	↑↓		↑

[a] $3d_\delta$ denotes the nonbonding MO localized on Mn.

The calculations of $MnO(P)^+$ were done with two active spaces used in our previous study.[46] The smallest active space consists of 16 to 18 orbitals containing 14 active electrons: four pairs of bonding/antibonding MOs between Mn(3d) and the ligand atoms, the nonbonding $Mn(3d_\delta)$ orbital, four porphyrin orbitals of the *Gouterman set*, $O(3p_x)$ and $O(3p_y)$ orbitals, and a maximum of three Mn(3d′) MOs $3d'_\delta$, $3d'_{xz}$, and $3d'_{yz}$. In the larger active space, an extra set of 12 $P(\pi)$ orbitals was added, resulting in a global active space of 28−30 orbitals containing 28 electrons (see ref 46). With the smaller active space, we used different m values from 100 to 1000, whereas with the larger one, only calculations with m = 1000, 2000, and 4000 were done.

In Table 7, we present the relative energies of the low-lying states of $MnO(P)^+$ calculated with DMRG-SCF(14,N)[m] and cu(4)-CASPT2(14,N)[m] with N = 16−18. We find a similar behavior in the cu(4)-CASPT2 results as compared to the other medium-sized active space calculations (NiFe hydrogenase, $Cr(CO)_6$, $Cu_2O_2^{2+}$), i.e. the cu(4)-CASPT2 results converge moderately. The differences between cu(4)-CASPT2[100] and cu(4)-CASPT2[1000] are less than 0.7 kcal/mol. The differences between the converged cu(4)-CASPT2[1000] and CASPT2 relative energies are modest, i.e. cu(4)-CASPT2 underestimates the $^5Mn^{IV}O(P^{\bullet}a_{1u})$−$^1Mn^{V}O(P)$ splitting by 1 kcal/mol while overestimating the $^3Mn^{V}O(P)$−$^1Mn^{V}O(P)$ splitting by 1.6 kcal/mol. Comparing all the results obtained so far with medium-sized active spaces, it seems that the 4-RDM approximation errors do increase somewhat with the size of the active space, leading to larger cu(4)-CASPT2 errors in $MnO(P)^+$, NiFe hydrogenase, and $Cr(CO)_6$ as compared to FeL_2 and Fe(P).

With the larger active space of 28−30 orbitals, a much larger m value is needed to get converged results. However, a cu(4)-CASPT2 calculation with m > 2000 is computationally too expensive as the memory requirement to calculate the 3-RDM becomes too demanding. Thus, in Table 8, we only present the DMRG-SCF results at m = 1000, 2000, and 4000 and the cu(4)-CASPT2 results at m = 1000 and 2000. With this large active space, both CASSCF/CASPT2 and CASPT2[m] calculations are computationally prohibited. Hence, RASSCF/RASPT2 results reported in our previous work[46] are used for comparison. The RASSCF results are not shown because the number of orbitals in RAS2 is different between the states, making the comparison between DMRG-SCF and RASSCF irrelevant.

As compared to the calculations with the smaller active spaces, we now find that the DMRG-SCF relative energies converge much slower. At m = 1000 the relative energies still differ by up to 1 kcal/mol with respect to the m = 4000 results, while the errors at m = 2000 are still around 0.1−0.4 kcal/mol. Thus, DMRG-SCF can only give results converged to within 0.1 kcal/mol at m larger than 2000.

The cu(4)-CASPT2 results are quite disappointing, i.e. the relative energies change by up to 1.8 kcal/mol going from m = 1000 to 2000. This indicates that even at m = 2000, the cu(4)-CASPT2 results have not yet converged, and it is expected that the relative energies could be changed at a larger m. Two strategies can be applied to solve this problem. The first solution is to improve the convergence of DMRG-SCF (e.g., by using a different orbital ordering), and (hope that this way) cu(4)-CASPT2 will converge at a smaller m. The second but not optimal solution is to further increase m to a higher value until stable cu(4)-CASPT2 results are obtained.

There are also some large discrepancies, 1.5 vs 3.9 kcal/mol, between best cu(4)-CASPT2[2000] and the RASPT2 results. Because in the two methods different approximation levels are employed, it is not trivial to conclude which of the two is more accurate. In RASPT2, more accurate results should be obtained by applying higher excitations between the subspaces (e.g., quadruple excitations) or by employing a larger RAS2. In cu(4)-CASPT2, m = 2000 does not seem high enough to obtain converged results. Moreover, cu(4)-CASPT2 contains an intrinsic error originating from the 4-RDM approximation. Because the number of 4-RDM elements scales as a^8, where a is the number of active orbitals, the number of approximated 4-RDM elements drastically increases with the size of the active space. Even if the error of each approximated 4-RDM element is small, overall these small errors can accumulate to a large total error.

4. CONCLUSION

In this work we have demonstrated how a (second-order) perturbational approach combined with DMRG, i.e. DMRG-cu(4)-CASPT2 and DMRG-CASPT2 can be used to study different problems in several transition metal complexes. The

Table 7. Relative Energies (kcal/mol) of the Low-Lying Electronic States of $MnO(P)^+$ Calculated with DMRG-SCF(14,N)[m] and cu(4)-CASPT2(14,N)[m] with N = 16, 17, or 18, in Comparison with CASSCF and CASPT2 Results[c]

	$^5Mn^{IV}O(P^{\bullet}a_{1u})$		$^5Mn^{IV}O(P^{\bullet}a_{2u})$		$^3Mn^{IV}O(P^{\bullet}a_{1u})$		$^3Mn^{IV}O(P^{\bullet}a_{2u})$		$^3Mn^{V}O(P)$	
m	SCF	PT2[b]	SCF	PT2[b]	SCF	PT2[b]	SCF	PT2[b]	SCF	PT2[b]
100	−21.3	20.2	−4.4	12.6	−17.4	22.7	0.0	16.2	−0.7	5.5
200	−21.4	20.5	−4.5	12.6	−17.6	23.8	−0.4	15.8	−0.7	5.9
400	−21.5	20.2	−4.6	12.6	−17.7	23.5	−0.5	15.9	−0.7	5.4
1000	−21.5	19.8	−4.6	12.5	−17.7	23.2	−0.5	16.9	−0.7	5.5
CAS[a]	−21.5	20.8	−4.6	13.0	−17.7	22.8	−0.5	15.8	−0.7	3.9

[a] CASSCF/CASPT2 from ref 46. [b] cu(4)-CASPT2. [c] The $^1Mn^{V}O(P)$ state is the reference.

DOI: 10.1021/acs.jctc.6b00714
J. Chem. Theory Comput. 2016, 12, 4352−4361

Table 8. Relative Energies (kcal/mol) of the Low-Lying Electronic States of $MnO(P)^+$ Calculated with DMRG-SCF(28,N)[m] and cu(4)-CASPT2(28,N)[m] with N = 28, 29, or 30, in Comparison with RASPT2 Results[c]

	$^5Mn^{IV}O(P^\bullet a_{1u})$		$^5Mn^{IV}O(P^\bullet a_{2u})$		$^3Mn^{IV}O(P^\bullet a_{1u})$		$^3Mn^{IV}O(P^\bullet a_{2u})$		$^3Mn^{V}O(P)$	
m	SCF	PT2[b]	SCF	PT2[b]	SCF	PT2[b]	SCF	PT2[b]	SCF	PT2[b]
1000	−37.4	16.7	−27.4	20.0	−32.4	23.5	−22.2	25.0	−3.8	7.7
2000	−37.8	18.2	−27.1	19.7	−33.0	24.0	−21.9	24.6	−4.0	9.5
4000	−37.9		−27.2		−33.4		−22.1		−4.1	
RAS[a]		19.5		18.3		22.0		21.9		5.6

[a]RASSCF/RASPT2 from ref 46. [b]cu(4)-CASPT2. [c]The $^1Mn^{V}O(P)$ state is the reference.

results in this work clearly point out that DMRG-SCF by itself is incapable of providing quantitative results, because it lacks dynamic correlation. In order to improve the results, we relied on either DMRG-cu(4)-CASPT2 (denoted as cu(4)-CASPT2-[m]), which has been recently developed and applied by Yanai et al.[22,32,41] or DMRG-CASPT2 (denoted as CASPT2[m]), which was implemented by Wouters et al.[33] in CheMPS2. These methods were employed to study the relative energies between different states of FeL_2, Fe(P), $Cr(CO)_6$, NiFe hydrogenase, and $MnO(P)^+$. Encouraging results were obtained, as cu(4)-CASPT2 can reproduce the CASPT2 results to within 0.1−0.2 kcal/mol in calculations with small active spaces and to within 2 kcal/mol for medium-sized active spaces. In the calculations of the electronic absorption spectrum of $Cr(CO)_6$, the errors are larger, 0.1−0.2 eV, but still acceptable for excited state calculations. In the calculations with the large active space in $MnO(P)^+$, the performance of cu(4)-CASPT2 is less impressive. Remaining errors originate from two sources: the finite m value and the 4-RDM approximation. The former errors can be eliminated by increasing m, but this can drastically increase the computational cost as the scaling of 3-RDM calculations is $O(a^4m^3 + a^6m^2)$.[32] For the time being we can only perform cu(4)-CASPT2(28,30)[m] calculations with m up to 2000. The 4-RDM approximation also introduces intrinsic errors into the cu(4)-CASPT2 solutions, and, unfortunately, the errors seem to be more pronounced with larger active spaces. Obviously, the solution is to explicitly calculate the 4-RDM, but this again is computationally expensive for large-sized active spaces. On the whole, our experience with the cu(4)-CASPT2 method is quite positive, in particular for calculations employing not too large active spaces (less than 24 orbitals).

■ ASSOCIATED CONTENT

Supporting Information

The Supporting Information is available free of charge on the ACS Publications website at DOI: 10.1021/acs.jctc.6b00714.

Cartesian coordinates of the molecules studied in this work (PDF)

■ AUTHOR INFORMATION

Corresponding Author

*E-mail: kristin.pierloot@kuleuven.be.

Notes

The authors declare no competing financial interest.

■ ACKNOWLEDGMENTS

This investigation has been supported by grants from the Flemish Science Foundation (FWO). The computational resources and services used in this work were provided by the VSC (Flemish Supercomputer Center), funded by the Research Foundation - Flanders (FWO) and the Flemish Government - department EWI. The authors thank Prof. N. Nakatani (Hokkaido University) for providing the interface between Molcas and Block.

■ REFERENCES

(1) White, S. R. *Phys. Rev. Lett.* **1992**, *69*, 2863.
(2) White, S. R. *Phys. Rev. B: Condens. Matter Mater. Phys.* **1993**, *48*, 10345.
(3) Olivares-Amaya, R.; Hu, W.; Nakatani, N.; Sharma, S.; Yang, J.; Chan, G. K.-L. *J. Chem. Phys.* **2015**, *142*, 034102.
(4) Schollwöck, U. *Ann. Phys.* **2011**, *326*, 96−192.
(5) Chan, G. K.-L.; Head-Gordon, M. *J. Chem. Phys.* **2003**, *118*, 8551−8554.
(6) Chan, G. K.-L.; Kállay, M.; Gauss, J. *J. Chem. Phys.* **2004**, *121*, 6110−6116.
(7) Sharma, S.; Yanai, T.; Booth, G. H.; Umrigar, C.; Chan, G. K.-L. *J. Chem. Phys.* **2014**, *140*, 104112.
(8) Kurashige, Y.; Yanai, T. *J. Chem. Phys.* **2009**, *130*, 234114.
(9) Yanai, T.; Kurashige, Y.; Neuscamman, E.; Chan, G. K.-L. *J. Chem. Phys.* **2010**, *132*, 024105.
(10) Marti, K. H.; Ondík, I. M.; Moritz, G.; Reiher, M. *J. Chem. Phys.* **2008**, *128*, 014104.
(11) Neuscamman, E.; Yanai, T.; Chan, G. K.-L. *J. Chem. Phys.* **2010**, *132*, 024106.
(12) Sharma, S.; Chan, G. K.-L. *J. Chem. Phys.* **2012**, *136*, 124121.
(13) Boguslawski, K.; Marti, K. H.; Legeza, O.; Reiher, M. *J. Chem. Theory Comput.* **2012**, *8*, 1970−1982.
(14) Boguslawski, K.; Tecmer, P.; Legeza, O.; Reiher, M. *J. Phys. Chem. Lett.* **2012**, *3*, 3129−3135.
(15) Kurashige, Y.; Chan, G. K.-L.; Yanai, T. *Nat. Chem.* **2013**, *5*, 660−666.
(16) Harris, T. V.; Kurashige, Y.; Yanai, T.; Morokuma, K. *J. Chem. Phys.* **2014**, *140*, 054303.
(17) Sharma, S.; Sivalingam, K.; Neese, F.; Chan, G. K.-L. *Nat. Chem.* **2014**, *6*, 927−933.
(18) Kurashige, Y.; Saitow, M.; Chalupský, J.; Yanai, T. *Phys. Chem. Chem. Phys.* **2014**, *16*, 11988−11999.
(19) Chalupský, J.; Rokob, T. A.; Kurashige, Y.; Yanai, T.; Solomon, E. I.; Rulíšek, L.; Srnec, M. *J. Am. Chem. Soc.* **2014**, *136*, 15977−15991.
(20) Wouters, S.; Bogaerts, T.; Van Der Voort, P.; Van Speybroeck, V.; Van Neck, D. *J. Chem. Phys.* **2014**, *140*, 241103.
(21) Freitag, L.; Knecht, S.; Keller, S. F.; Delcey, M. G.; Aquilante, F.; Pedersen, T. B.; Lindh, R.; Reiher, M.; González, L. *Phys. Chem. Chem. Phys.* **2015**, *17*, 14383−14392.
(22) Saitow, M.; Kurashige, Y.; Yanai, T. *J. Chem. Theory Comput.* **2015**, *11*, 5120−5131.
(23) Legeza, O.; Sólyom, J. *Phys. Rev. B: Condens. Matter Mater. Phys.* **2003**, *68*, 195116.
(24) Boguslawski, K.; Tecmer, P.; Barcza, G.; Legeza, O.; Reiher, M. *J. Chem. Theory Comput.* **2013**, *9*, 2959−2973.
(25) Mottet, M.; Tecmer, P.; Boguslawski, K.; Legeza, Ö.; Reiher, M. *Phys. Chem. Chem. Phys.* **2014**, *16*, 8872−8880.
(26) Stein, C. J.; Reiher, M. *J. Chem. Theory Comput.* **2016**, *12*, 1760−1771.

DOI: 10.1021/acs.jctc.6b00714
J. Chem. Theory Comput. 2016, 12, 4352−4361

(27) Barcza, G.; Legeza, Ö.; Marti, K.; Reiher, M. *Phys. Rev. A: At., Mol., Opt. Phys.* **2011**, *83*, 012508.
(28) Moritz, G.; Hess, B. A.; Reiher, M. *J. Chem. Phys.* **2005**, *122*, 024107.
(29) Chan, G. K.-L.; Head-Gordon, M. *J. Chem. Phys.* **2002**, *116*, 4462−4476.
(30) Andersson, K.; Malmqvist, P.-Å.; Roos, B. O. *J. Chem. Phys.* **1992**, *96*, 1218−1226.
(31) Kurashige, Y.; Yanai, T. *J. Chem. Phys.* **2011**, *135*, 094104.
(32) Kurashige, Y.; Chalupský, J.; Lan, T. N.; Yanai, T. *J. Chem. Phys.* **2014**, *141*, 174111.
(33) Wouters, S.; Van Speybroeck, V.; Van Neck, D. *J. Chem. Phys.* **2016**, *145*, 054120.
(34) Angeli, C.; Cimiraglia, R.; Evangelisti, S.; Leininger, T.; Malrieu, J.-P. *J. Chem. Phys.* **2001**, *114*, 10252−10264.
(35) Angeli, C.; Cimiraglia, R.; Malrieu, J.-P. *J. Chem. Phys.* **2002**, *117*, 9138−9153.
(36) Angeli, C.; Pastore, M.; Cimiraglia, R. *Theor. Chem. Acc.* **2007**, *117*, 743−754.
(37) Sharma, S.; Chan, G. K.-L. *J. Chem. Phys.* **2014**, *141*, 111101.
(38) Guo, S.; Watson, M. A.; Hu, W.; Sun, Q.; Chan, G. K.-L. *J. Chem. Theory Comput.* **2016**, *12*, 1583−1591.
(39) Knecht, S.; Hedegård, E. D.; Keller, S.; Kovyrshin, A.; Ma, Y.; Muolo, A.; Stein, C. J.; Reiher, M. *Chimia* **2016**, *70*, 244−251.
(40) Roemelt, M.; Guo, S.; Chan, G. K.-L. *J. Chem. Phys.* **2016**, *144*, 204113.
(41) Shirai, S.; Kurashige, Y.; Yanai, T. *J. Chem. Theory Comput.* **2016**, *12*, 2366−2372.
(42) Zgid, D.; Ghosh, D.; Neuscamman, E.; Chan, G. K.-L. *J. Chem. Phys.* **2009**, *130*, 194107.
(43) Malmqvist, P.-Å.; Pierloot, K.; Shahi, A. R. M.; Cramer, C. J.; Gagliardi, L. *J. Chem. Phys.* **2008**, *128*, 204109.
(44) Vancoillie, S.; Zhao, H.; Tran, V. T.; Hendrickx, M. F. A.; Pierloot, K. *J. Chem. Theory Comput.* **2011**, *7*, 3961−3977.
(45) Delcey, M. G.; Pierloot, K.; Phung, Q. M.; Vancoillie, S.; Lindh, R.; Ryde, U. *Phys. Chem. Chem. Phys.* **2014**, *16*, 7927−7938.
(46) Venturinelli Jannuzzi, S. A.; Phung, Q. M.; Domingo, A.; Formiga, A. L. B.; Pierloot, K. *Inorg. Chem.* **2016**, *55*, 5168.
(47) In the beginning of 2015 an error was discovered in the ANO-RCC basis set of C, included in MOLCAS versions 6.4−8.0, see http://www.molcas.org/ANO/indexC.html. The corrected C basis set is used in this work, whereas previous works before 2015 employed the faulty basis set. Small test calculations have shown that the errors are not negligible even for very large contractions.
(48) Wouters, S.; Poelmans, W.; Ayers, P. W.; Van Neck, D. *Comput. Phys. Commun.* **2014**, *185*, 1501−1514.
(49) Wouters, S.; Van Neck, D. *Eur. Phys. J. D* **2014**, *68*, 272.
(50) Aquilante, F.; Autschbach, J.; Carlson, R. K.; Chibotaru, L. F.; Delcey, M. G.; De Vico, L.; Fdez. Galván, I.; Ferré, N.; Frutos, L. M.; Gagliardi, L.; Garavelli, M.; Giussani, A.; Hoyer, C. E.; Li Manni, G.; Lischka, H.; Ma, D.; Malmqvist, P. k.; Müller, T.; Nenov, A.; Olivucci, M.; Pedersen, T. B.; Peng, D.; Plasser, F.; Pritchard, B.; Reiher, M.; Rivalta, I.; Schapiro, I.; Segarra-Martí, J.; Stenrup, M.; Truhlar, D. G.; Ungur, L.; Valentini, A.; Vancoillie, S.; Veryazov, V.; Vysotskiy, V. P.; Weingart, O.; Zapata, F.; Lindh, R. *J. Comput. Chem.* **2016**, *37*, 506−541.
(51) Chan, G. K.-L. *J. Chem. Phys.* **2004**, *120*, 3172−3178.
(52) Ghosh, D.; Hachmann, J.; Yanai, T.; Chan, G. K.-L. *J. Chem. Phys.* **2008**, *128*, 144117.
(53) Zgid, D.; Nooijen, M. *J. Chem. Phys.* **2008**, *128*, 014107.
(54) Roos, B. O.; Lindh, R.; Malmqvist, P.-Å; Veryazov, V.; Widmark, P.-O. *J. Phys. Chem. A* **2005**, *109*, 6575−6579.
(55) Roos, B. O.; Lindh, R.; Malmqvist, P.-Å; Veryazov, V.; Widmark, P.-O. *J. Phys. Chem. A* **2004**, *108*, 2851−2858.
(56) Widmark, P.-O.; Malmqvist, P.-Å; Roos, B. O. *Theor. Chem. Acc.* **1990**, *77*, 291−306.
(57) Hess, B. A. *Phys. Rev. A: At., Mol., Opt. Phys.* **1986**, *33*, 3742−3748.
(58) Reiher, M.; Wolf, A. *J. Chem. Phys.* **2004**, *121*, 2037−2047.
(59) Reiher, M.; Wolf, A. *J. Chem. Phys.* **2004**, *121*, 10945−10956.
(60) Ghigo, G.; Roos, B. O.; Malmqvist, P.-Å. *Chem. Phys. Lett.* **2004**, *396*, 142−149.
(61) Forsberg, N.; Malmqvist, P.-Å. *Chem. Phys. Lett.* **1997**, *274*, 196−204.
(62) Aquilante, F.; Malmqvist, P.-Å; Pedersen, T. B.; Ghosh, A.; Roos, B. O. *J. Chem. Theory Comput.* **2008**, *4*, 694−702.
(63) Radoń, M. *J. Chem. Theory Comput.* **2014**, *10*, 2306−2321.
(64) Rees, B.; Mitschler, A. *J. Am. Chem. Soc.* **1976**, *98*, 7918−7924.
(65) Collman, J. P.; Hoard, J.; Kim, N.; Lang, G.; Reed, C. A. *J. Am. Chem. Soc.* **1975**, *97*, 2676−2681.
(66) Goff, H.; La Mar, G. N.; Reed, C. A. *J. Am. Chem. Soc.* **1977**, *99*, 3641−3646.
(67) Kitagawa, T.; Teraoka, J. *Chem. Phys. Lett.* **1979**, *63*, 443−446.
(68) Dolphin, D.; Sams, J. R.; Tsin, T. B.; Wong, K. L. *J. Am. Chem. Soc.* **1976**, *98*, 6970−6975.
(69) Lang, G.; Spartalian, K.; Reed, C. A.; Collman, J. P. *J. Chem. Phys.* **1978**, *69*, 5424−5427.
(70) Boyd, P. D.; Buckingham, D. A.; McMeeking, R. F.; Mitra, S. *Inorg. Chem.* **1979**, *18*, 3585−3591.
(71) Mispelter, J.; Momenteau, M.; Lhoste, J. *J. Chem. Phys.* **1980**, *72*, 1003−1012.
(72) Strauss, S. H.; Silver, M. E.; Long, K. M.; Thompson, R. G.; Hudgens, R. A.; Spartalian, K.; Ibers, J. A. *J. Am. Chem. Soc.* **1985**, *107*, 4207−4215.
(73) Pierloot, K. *Mol. Phys.* **2003**, *101*, 2083−2094.
(74) Radoń, M.; Pierloot, K. *J. Phys. Chem. A* **2008**, *112*, 11824−11832.
(75) Scherlis, D. A.; Estrin, D. A. *Int. J. Quantum Chem.* **2002**, *87*, 158−166.
(76) Liao, M.-S.; Scheiner, S. *J. Chem. Phys.* **2002**, *117*, 205−219.
(77) Deeth, R. J.; Fey, N. *J. Comput. Chem.* **2004**, *25*, 1840−1848.
(78) Groenhof, A. R.; Swart, M.; Ehlers, A. W.; Lammertsma, K. *J. Phys. Chem. A* **2005**, *109*, 3411−3417.
(79) Liao, M.-S.; Watts, J. D.; Huang, M.-J. *J. Phys. Chem. A* **2007**, *111*, 5927−5935.
(80) Khvostichenko, D.; Choi, A.; Boulatov, R. *J. Phys. Chem. A* **2008**, *112*, 3700−3711.
(81) Vancoillie, S.; Radoń, M.; Zhao, H.; Pierloot, K. *J. Chem. Theory Comput.* **2010**, *6*, 576−582.
(82) Pierloot, K.; Phung, Q. M.; Domingo, A. to be published.
(83) Rosa, A.; Baerends, E. J.; van Gisbergen, S. J.; van Lenthe, E.; Groeneveld, J. A.; Snijders, J. G. *J. Am. Chem. Soc.* **1999**, *121*, 10356−10365.
(84) Hummel, P.; Oxgaard, J.; Goddard, W. A.; Gray, H. B. *Inorg. Chem.* **2005**, *44*, 2454−2458.
(85) Ben Amor, N.; Villaume, S.; Maynau, D.; Daniel, C. *Chem. Phys. Lett.* **2006**, *421*, 378−382.
(86) Villaume, S.; Strich, A.; Daniel, C.; Perera, S. A.; Bartlett, R. J. *Phys. Chem. Chem. Phys.* **2007**, *9*, 6115−6122.
(87) Beach, N. A.; Gray, H. B. *J. Am. Chem. Soc.* **1968**, *90*, 5713−5721.
(88) Gray, H. B.; Beach, N. *J. Am. Chem. Soc.* **1963**, *85*, 2922−2927.
(89) Fontecilla-Camps, J. C.; Volbeda, A.; Cavazza, C.; Nicolet, Y. *Chem. Rev.* **2007**, *107*, 4273−4303.
(90) Volbeda, A.; Fontecilla-Camps, J. C. *Coord. Chem. Rev.* **2005**, *249*, 1609−1619.
(91) De Lacey, A. L.; Fernandez, V. M.; Rousset, M.; Cammack, R. *Chem. Rev.* **2007**, *107*, 4304−4330.
(92) Lubitz, W.; Reijerse, E.; van Gastel, M. *Chem. Rev.* **2007**, *107*, 4331−4365.
(93) Vincent, K. A.; Parkin, A.; Armstrong, F. A. *Chem. Rev.* **2007**, *107*, 4366−4413.
(94) Siegbahn, P. E. M.; Tye, J. W.; Hall, M. B. *Chem. Rev.* **2007**, *107*, 4414−4435.
(95) Cramer, C. J.; Włoch, M.; Piecuch, P.; Puzzarini, C.; Gagliardi, L. *J. Phys. Chem. A* **2006**, *110*, 1991−2004.
(96) Yachandra, V. K.; Sauer, K.; Klein, M. P. *Chem. Rev.* **1996**, *96*, 2927−2950.

DOI: 10.1021/acs.jctc.6b00714
J. Chem. Theory Comput. 2016, 12, 4352−4361

(97) Groves, J. T.; Lee, J.; Marla, S. S. *J. Am. Chem. Soc.* **1997**, *119*, 6269−6273.
(98) Jin, N.; Groves, J. T. *J. Am. Chem. Soc.* **1999**, *121*, 2923−2924.
(99) Song, W. J.; Seo, M. S.; DeBeer George, S.; Ohta, T.; Song, R.; Kang, M.-J.; Tosha, T.; Kitagawa, T.; Solomon, E. I.; Nam, W. *J. Am. Chem. Soc.* **2007**, *129*, 1268−1277.
(100) Jin, N.; Ibrahim, M.; Spiro, T. G.; Groves, J. T. *J. Am. Chem. Soc.* **2007**, *129*, 12416−12417.
(101) Balcells, D.; Raynaud, C.; Crabtree, R. H.; Eisenstein, O. *Chem. Commun.* **2008**, 744−746.
(102) Balcells, D.; Raynaud, C.; Crabtree, R. H.; Eisenstein, O. *Inorg. Chem.* **2008**, *47*, 10090−10099.

DOI: 10.1021/acs.jctc.6b00714
J. Chem. Theory Comput. 2016, 12, 4352−4361